

This article was downloaded by: [Haemmerich, Dieter]

On: 2 April 2009

Access details: Access Details: [subscription number 910059635]

Publisher Informa Healthcare

Informa Ltd Registered in England and Wales Registered Number: 1072954 Registered office: Mortimer House, 37-41 Mortimer Street, London W1T 3JH, UK



International Journal of Hyperthermia

Publication details, including instructions for authors and subscription information:

<http://www.informaworld.com/smpp/title~content=t713599996>

Effect of electrode thermal conductivity in cardiac radiofrequency catheter ablation: A computational modeling study

David Schutt ^a; Enrique J. Berjano ^b; Dieter Haemmerich ^c

^a Medical University of South Carolina, Charleston, South Carolina ^b Institute for Research and Innovation on Bioengineering, Valencia Polytechnic University, Valencia, Spain ^c Pediatric Cardiology, Medical University of South Carolina, Charleston, South Carolina

Online Publication Date: 01 March 2009

To cite this Article Schutt, David, Berjano, Enrique J. and Haemmerich, Dieter(2009)'Effect of electrode thermal conductivity in cardiac radiofrequency catheter ablation: A computational modeling study',International Journal of Hyperthermia,25:2,99 — 107

To link to this Article: DOI: 10.1080/02656730802563051

URL: <http://dx.doi.org/10.1080/02656730802563051>

PLEASE SCROLL DOWN FOR ARTICLE

Full terms and conditions of use: <http://www.informaworld.com/terms-and-conditions-of-access.pdf>

This article may be used for research, teaching and private study purposes. Any substantial or systematic reproduction, re-distribution, re-selling, loan or sub-licensing, systematic supply or distribution in any form to anyone is expressly forbidden.

The publisher does not give any warranty express or implied or make any representation that the contents will be complete or accurate or up to date. The accuracy of any instructions, formulae and drug doses should be independently verified with primary sources. The publisher shall not be liable for any loss, actions, claims, proceedings, demand or costs or damages whatsoever or howsoever caused arising directly or indirectly in connection with or arising out of the use of this material.

Effect of electrode thermal conductivity in cardiac radiofrequency catheter ablation: A computational modeling study

DAVID SCHUTT¹, ENRIQUE J. BERJANO², & DIETER HAEMMERICH³

¹Medical University of South Carolina, Charleston, South Carolina, ²Institute for Research and Innovation on Bioengineering, Valencia Polytechnic University, Valencia, Spain and ³Pediatric Cardiology, Medical University of South Carolina, Charleston, South Carolina

(Received 7 August 2008; Revised 13 October 2008; Accepted 17 October 2008)

Abstract

Purpose: Radiofrequency (RF ablation) is the treatment of choice for certain types of cardiac arrhythmias. Recent studies have suggested that using gold instead of platinum as the electrode material for cardiac catheter ablation leads to larger thermal lesions due to its higher thermal conductivity. In this study we created computer models to compare the effects of different electrode materials on lesion dimensions using different catheters, insertion depths, and flow rates.

Materials and methods: Finite element method (FEM) models of two cardiac ablation electrodes (7Fr, length 4 mm and 8Fr, length 10 mm) made of platinum, gold, and copper were created with tissue insertion depths of 0.75, 1.25, and 2.5 mm. Convective cooling was applied to the electrode and tissue based on measurements from previous studies at different flow rates. RF ablations were simulated with both temperature control and constant power control algorithms to determine temperature profiles after 60 s.

Results: With the constant power algorithm there was no difference in lesion dimensions between the electrode materials over the range of parameters. With the temperature control algorithm, lesion width and depth were only marginally larger (~0.1–0.7 mm) with the gold and copper electrodes compared to the platinum electrode for all parameter combinations.

Conclusion: Our computer modelling results show only minor increases in thermal lesion dimensions with electrode materials of higher thermal conductivity. These observed differences likely do not provide a significant advantage during clinical procedures.

Keywords: Ablation, cardiac ablation, electrode thermal conductivity, radiofrequency ablation, theoretical modeling

Introduction

Radiofrequency (RF) ablation has become the treatment of choice for certain types of cardiac arrhythmias. For cardiac RF ablation (also known as cardiac catheter ablation), different technologies have been developed in an attempt to increase the thermal lesion dimensions to ensure adequate ablation of the target region, including internally cooled catheters, open-perfusion catheters, and large-tip catheters [1–6]. Several studies have investigated the effect of the use of different catheter tip (i.e. electrode) materials on thermal lesion size due to varying thermal properties of these materials, including both ex-vivo [7, 8] and clinical studies [9, 10].

These studies compared standard electrodes made of platinum-iridium (Pt-Ir) to electrodes made of gold (Au), which has a higher thermal conductivity (k). Higher thermal conductivity of the electrode is theoretically desirable since it allows more heat conduction along the electrode from the electrode-tissue interface to the electrode-blood interface (where the heat is removed convectively). This increased cooling of the electrode-tissue interface allows greater power to be applied for a given target tip temperature during the ablation. Although ex vivo results showed that the use of gold electrodes led to larger thermal lesions [7, 8], clinical studies did not demonstrate any significant difference between the

two electrode materials in terms of applied power, tip temperature or clinical outcome [9, 10].

The goal of the current study was to investigate the effect of different catheter tip materials on thermal lesion size using computer models. Variations in parameters such as electrode length, insertion depth of the electrode into the tissue, and flow rate of the circulating blood (i.e. the amount of convective cooling) may all affect the comparative performance between electrodes of different materials and were evaluated. Additionally, since thermal lesion dimensions may depend on the energy control algorithm that is used (both temperature control and constant power algorithms are commonly used in clinical application), we performed simulations with both energy control algorithms for comparison.

Although our results are particular to the case of cardiac RF ablation, they may also have significance for other RF ablation applications such as heating of the cornea, where prior studies showed that the thermal conductivity of the electrode significantly affects the temperature profile [11].

Numerical model

Description of the theoretical model

During cardiac RF ablation, electrical current flows between the active electrode at the catheter tip and a large dispersive electrode located on the patient's back. Although the active electrode may be located at varying angles to the endocardium surface, our study considered the case where the electrode is perpendicular to and partially inserted into the endocardial tissue (Figure 1). The geometry of this configuration allowed the use of an axisymmetric two-dimensional model.

We included an embedded thermistor at the tip of the electrode for temperature control simulation similar to a previous study [12]. Table I shows the value of the physical properties used in the model, which were taken from the literature [13–17]. We considered a change in the electrical conductivity of the cardiac tissue of $+1.5\%/^{\circ}\text{C}$ [13], and included temperature dependent effects on the thermal conductivity and specific heat of cardiac tissue as published previously [14].

Electrode thermal conductivity in RF ablation

The initial temperature in the entire model was 37°C . Likewise, the temperature at the outer model boundaries was set to 37°C . We used convective film coefficients with a sink temperature of 37°C to model the convective heat transfer at both the blood–endocardium and blood–electrode interfaces. The film coefficients were varied according to typical

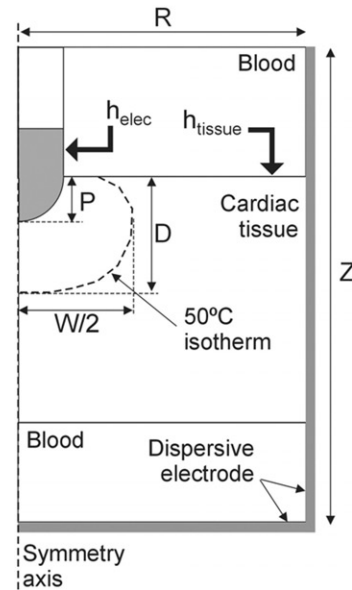


Figure 1. Diagram of axisymmetric model geometry (not to scale). RF electrical current flows between the active electrode and a large dispersive electrode. The active electrode had a hemispherical tip and was inserted in the cardiac tissue up to a depth P . The value of the model parameters R and Z were determined using sensitivity analysis to avoid boundary effects ($R = 100\text{ mm}$, $Z = 140\text{ mm}$). Lesion dimensions (depth D and width W) were assessed using the 50°C isotherm line.

blood flow velocities in the heart (see below). Since the temperature of the blood was assumed to be a constant 37°C , we ignored the effects of heat conduction into the blood and did not include its thermal properties in the model.

The temperature distributions were calculated using the finite element method (FEM). ABAQUS/STANDARD 6.5 FEM solver software (Hibbitt, Karlsson & Sorensen, Inc., Pawtucket, RI) was used for all computer simulations. We obtained the temperature distribution in the tissue by solving the heat transfer equation (Equation 1), where we ignored both blood perfusion heat loss (Q_p) and metabolic heat generation (Q_m) due to their relatively small magnitudes [12]:

$$\rho c \frac{\partial T}{\partial t} = \nabla \cdot k \nabla T + q - Q_p + Q_m \quad (1)$$

where ρ is the density, c is the specific heat, k is the thermal conductivity and q is the heat source term resulting from RF power deposition. The electrical field problem was solved using Laplace's equation:

$$\nabla \cdot \sigma \nabla V = 0 \quad (2)$$

where V is the voltage and σ is the electrical conductivity. The electric potential at the distal model boundary (i.e. the dispersive electrode) was 0 V .

Table I. Model material properties at 37°C.

Material	Region	c (J/kg K)	k (W/m K)	σ (S/m)	ρ (kg/m ³)
Blood	Blood	NA	NA	0.667	NA
Myocardium	Tissue	3111	0.531	0.541	1.06·10 ³
Pt-Ir	Electrode	132	71	4.10 ⁶	21.5·10 ³
Au	Electrode	129	317	45.0 ⁶	19.3·10 ³
Cu	Electrode	384	401	60.10 ⁶	9.0·10 ³
Polyurethane	Catheter body	1045	0.026	10 ⁻⁵	70
Glass fiber	Thermistor	835	71	10 ⁻⁵	32
Insulation	Thermistor	835	0.038	10 ⁻⁵	32

Construction of the model

We used PATRAN 2005 r2 (The MacNeal-Schwendler Co., Los Angeles, CA) to create the model geometry, perform meshing, and assign temperature and voltage boundary conditions. The node spacing in the model was spatially heterogeneous: the finest mesh was at the electrode–tissue interface because the largest voltage and temperature gradients appear at this location. The mesh grid size increased gradually with distance from the electrode–tissue from ~0.1 mm in the tissue near the electrode to ~10 mm at the distal model boundary.

Parametric studies

We considered two different clinical catheter types in this study: a 7Fr (2.33 mm diameter) catheter with an electrode length of 4 mm, and an 8Fr (2.67 mm diameter) catheter with an electrode length of 10 mm. The effect of the circulating blood flow at the electrode and endocardium surfaces was modeled via convective film coefficients h_{elec} and h_{tissue} , assigned as boundary condition at these surfaces (Figure 1). By taking into account previous experimental measurements at different locations inside the cardiac chamber [18], h_{tissue} was varied between 44 and 1417 W/m²K. To determine the corresponding convective film coefficient values for the blood–electrode interface (h_{elec}), we first used Equation 3 to calculate blood velocity v (m/s):

$$v = \left(\frac{h_{tissue}}{h_{ref}} \right)^{1.25} \cdot v_{ref} \quad (3)$$

where h_{tissue} was the convective film coefficient at the blood–endocardium interface for the specified flow type (low, medium, or high (Table II)) and h_{ref} is a previously reported film coefficient value (1417 W/m²K⁴) at the blood velocity v_{ref} (0.244 m/s) [18]. We then used the calculated blood velocity v in Equations 4 to 7 to determine the convective film coefficient at the electrode–blood interface for both

Table II. Values of convective thermal coefficient h_{elec} and h_{tissue} used in this study. The values of h_{tissue} at ‘low’ and ‘high’ flow were taken from Tungjitkusolmun et al. [18]. The value of h_{tissue} at the ‘medium’ flow condition was taken as half of the value for ‘high’ flow. All values of h are in W/m²K⁴.

Flow type	h_{tissue}	h_{elec} (7Fr-cath)	h_{elec} (8Fr-cath)	Flow rate (cm/s)
Low	44	721	675	0.3
Medium	708	3636	3405	10.3
High	1417	5446	5101	24.4

catheter diameters [18]:

$$h_{elec} = \frac{Nu \cdot k}{d} \quad (4)$$

where Nu represents the Nusselt number, calculated in Equation 5:

$$Nu = 0.683 \cdot Re^{0.466} \cdot Pr^{0.333} \quad (5)$$

In Equation 5, Re and Pr represent the Reynolds and Prandtl numbers, and are calculated using Equations 6 and 7:

$$Re = \frac{\rho \cdot v \cdot d}{u} \quad (6)$$

$$Pr = \frac{c \cdot u}{k} \quad (7)$$

where k is the thermal conductivity of blood (0.543 W/(m·K)), d is the catheter diameter (2.33 (7Fr) or 2.66 (8Fr) mm), ρ is the density of blood (1060 kg/m³), u is the viscosity of blood (2.1·10⁻³ kg/(m·s)), and c is the specific heat of blood (3760 J/(kg K)).

The values of h_{elec} and h_{tissue} for the three simulated flow conditions are shown in Table II.

Finally, we examined three different electrode insertion depths (parameter P in Figure 1): 0.75, 1.25 and 2.5 mm.

Protocols of delivering radiofrequency energy

In this study, two algorithms for delivering RF energy were considered: temperature control and constant power. The first algorithm was implemented using an automatic feedback algorithm [19] with a target tip temperature of 55°C for 60 s. For the second algorithm, the applied voltage was adjusted during the trial to maintain a constant power for 60 s. The target value of constant power for each trial was determined from the results of the temperature control experiments, in that we used the lowest average power for a given electrode size, insertion depth, and flow rate (see Table III for further explanation).

Assessment of thermal lesion dimensions

Since myocardial injury occurs once the temperature reaches approximately 50°C [20] and there is no data on the time–temperature relationship of myocardial tissue damage, we used the 50°C isotherm to demarcate the thermal lesion boundary for all simulations. We compared the maximum width and depth of the thermal lesions (W and D in Figure 1 respectively), and the maximal temperature reached in the tissue (T_{\max}).

Results

The temperature distribution for a typical simulation is shown in Figure 2.

The results of all simulations with the 7Fr and 8Fr catheter and the temperature control algorithm are shown in Tables III and IV. The lesion dimensions from simulations with the Cu electrode are omitted from the results since they were similar (<0.1 mm difference) to lesion dimensions with the Au electrode for all cases.

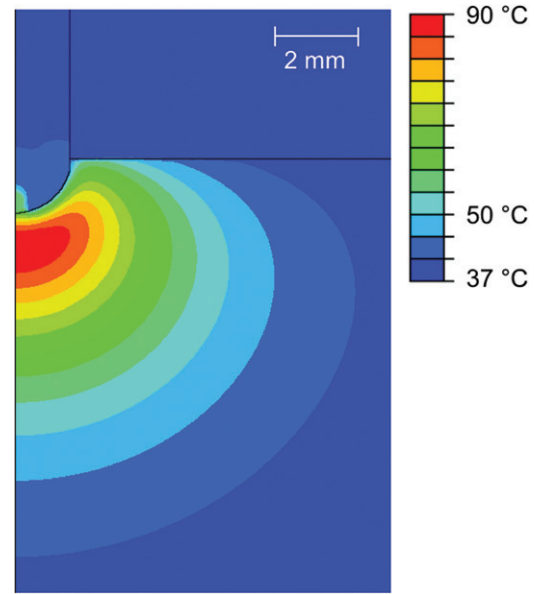


Figure 2. Detail view of temperature distribution after 60 s for a typical 8Fr catheter simulation. In this example, the electrode penetration depth was 1.25 mm and the flow rate was medium (Table II).

Table III. Results from simulations with 7Fr catheter and temperature control algorithm (55°C target temperature, 1 min duration).

Electrode material	Insertion depth	Flow type	Average power (W)	Max tissue temp (°C)	Lesion width	Lesion depth
Pt	0.75	low	3.53	68.2	8.3	4.3
Pt	0.75	medium	6.32	83.9	8.3	5.4
Pt	0.75	high	6.93	86.9	8.3	5.6
Au	0.75	low	3.65	68.9	8.5	4.4
Au	0.75	medium	6.58	87.4	8.6	5.6
Au	0.75	high	7.46	90.7	8.6	5.8
Pt	1.25	low	2.68	62.7	7.7	4.2
Pt	1.25	medium	5.05	77.2	8.1	5.5
Pt	1.25	high	5.62	80.5	8.2	5.7
Au	1.25	low	2.77	63.5	7.9	4.3
Au	1.25	medium	5.52	80.4	8.6	5.7
Au	1.25	high	6.20	84.5	8.7	6.0
Pt	2.5	low	1.69	57.7	7.0	4.5
Pt	2.5	medium	3.33	67.4	7.9	5.9
Pt	2.5	high	3.89	70.9	8.4	6.3
Au	2.5	low	1.72	57.8	7.1	4.6
Au	2.5	medium	3.54	68.8	8.3	6.1
Au	2.5	high	4.21	73.2	8.7	6.5

Note: All distance measurements are in mm. The lowest value of average power for each insertion depth and flow rate was used as the set power for the constant power algorithm simulation with those parameters (e.g. 3.53 W for 0.75 insertion depth and low flow).

The results of the temperature control simulations with both catheter sizes are shown graphically in Figures 3 to 6.

The results for the simulations with the constant power algorithm are shown in Table V. There was no appreciable difference in the thermal lesion dimensions between the different electrode materials using this algorithm for either catheter size (<0.1 mm for all cases).

The average initial impedance for the trials with the 7Fr catheter was 81, 82, and 85 ohms for the 0.75, 1.25, and 2.5 mm insertion depths, respectively.

The average initial impedance for the 8Fr catheter trials was 45, 46, and 46 ohms for the 0.75, 1.25, and 2.5 mm insertion depths.

Discussion

Previous ex vivo and clinical studies have investigated the effect of using Au instead of Pt-Ir as the electrode material for cardiac RF ablation, although the results of these studies were inconclusive; while the ex vivo studies demonstrated larger thermal

Table IV. Results from simulations with 8Fr catheter and temperature control algorithm (55°C target temperature, 1 min duration).

Electrode material	Insertion depth	Flow type	Average power (W)	Max tissue temp (°C)	Lesion width	Lesion depth
Pt	0.75	low	10.95	80.4	11.5	5.8
Pt	0.75	medium	15.86	93.8	10.5	6.7
Pt	0.75	high	16.75	95.4	10.2	6.7
Au	0.75	low	11.72	83.4	11.9	6.0
Au	0.75	medium	17.32	99.2	11.1	6.9
Au	0.75	high	18.30	99.7	10.9	7.0
Pt	1.25	low	9.16	73.9	11.1	5.8
Pt	1.25	medium	13.87	88.3	10.6	6.9
Pt	1.25	high	14.68	90.4	10.5	7.0
Au	1.25	low	9.82	76.1	11.5	6.0
Au	1.25	medium	15.44	94.3	11.3	7.2
Au	1.25	high	16.35	96.6	11.2	7.3
Pt	2.5	low	7.01	66.8	10.8	6.4
Pt	2.5	medium	11.46	82.0	11.3	7.7
Pt	2.5	high	12.28	84.7	11.4	7.9
Au	2.5	low	7.51	68.4	11.2	6.5
Au	2.5	medium	13.10	87.9	12.1	8.1
Au	2.5	high	14.17	91.6	12.2	8.4

Note: All distance measurements are in mm.

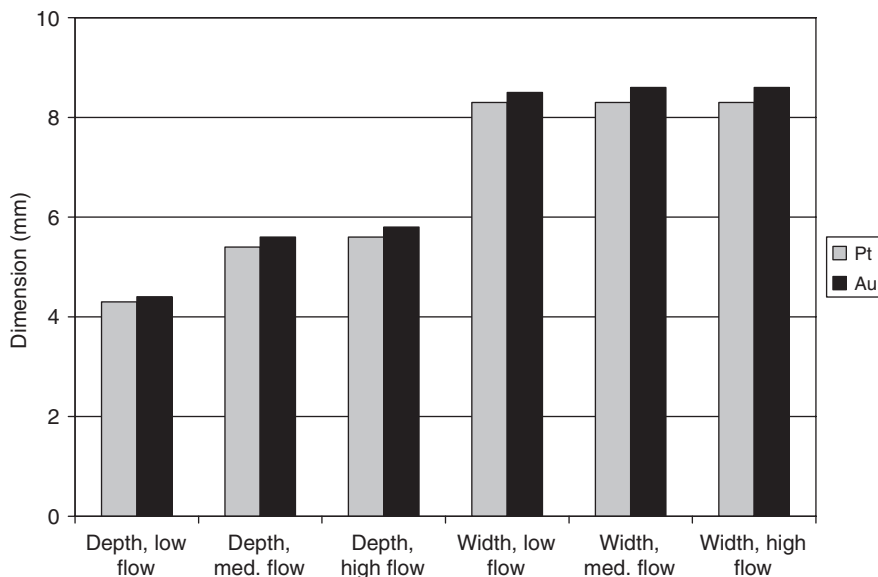


Figure 3. Comparison of lesion dimensions for the 7Fr catheter with 0.75 mm insertion depth.

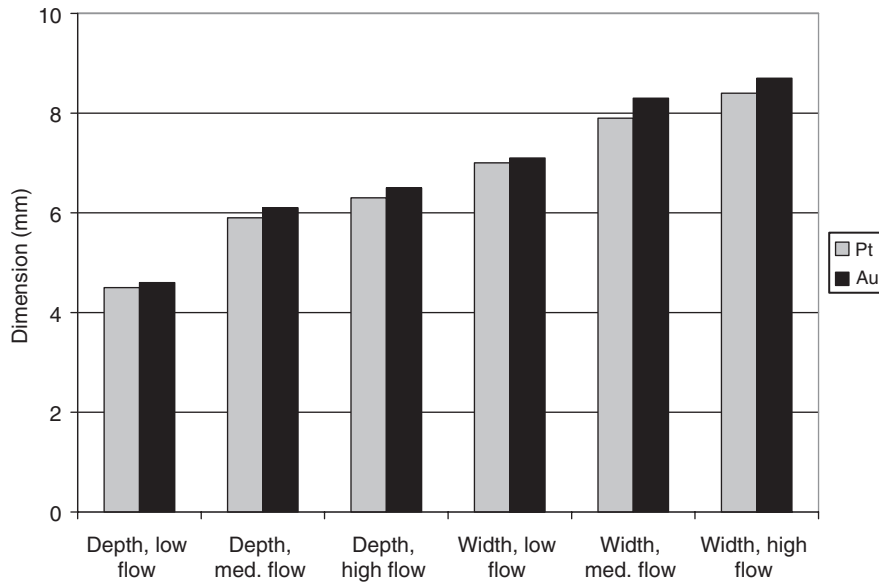


Figure 4. Comparison of lesion dimensions for the 7Fr catheter with 2.5 mm insertion depth.

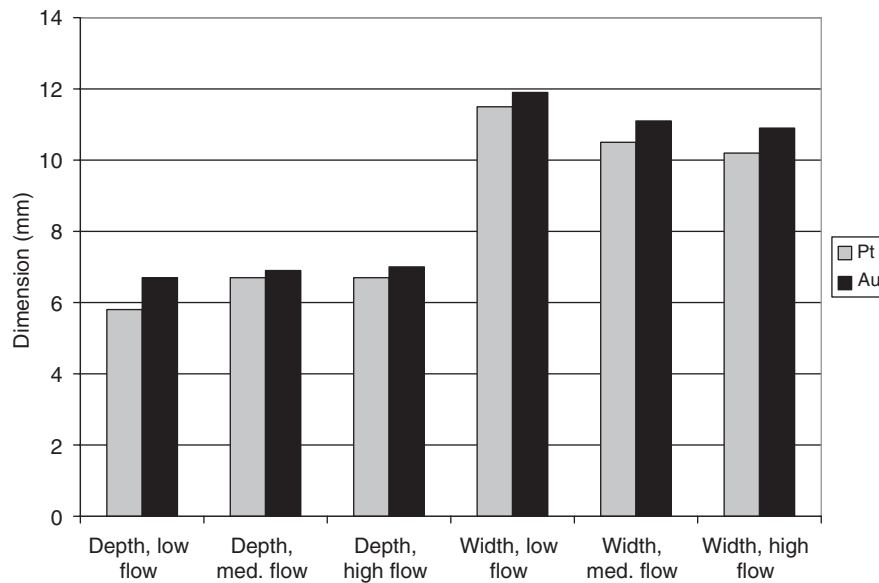


Figure 5. Comparison of lesion dimensions for the 8Fr catheter with 0.75 mm insertion depth.

lesions with Au electrodes [7, 8], clinical studies have not shown any significant differences in applied power, tip temperature, or clinical outcome between ablations with the two electrode materials [9, 10].

In this study we used computer models to investigate whether Au and Cu electrodes create larger thermal lesions than Pt-Ir electrodes using different catheter sizes and insertion depths at different flow conditions. With the temperature control algorithm we found that higher power was delivered with the Au and Cu electrodes in all simulations, resulting in higher maximum tissue temperatures but only slightly larger lesion

dimensions with both catheter sizes. We found no difference in lesion dimensions between the two electrode materials in the constant power algorithm simulations. Thus, while we saw an increase in applied power when using the constant temperature algorithm (Tables III and IV) due to the additional electrode cooling, this did not translate into significantly larger lesion dimensions.

It is well known that lesion dimensions increase with increasing flow when performing ablations with a temperature control algorithm [21], and generally we observed this effect in our simulations (Tables III and IV, Figures 3 to 6). The exceptions to this rule

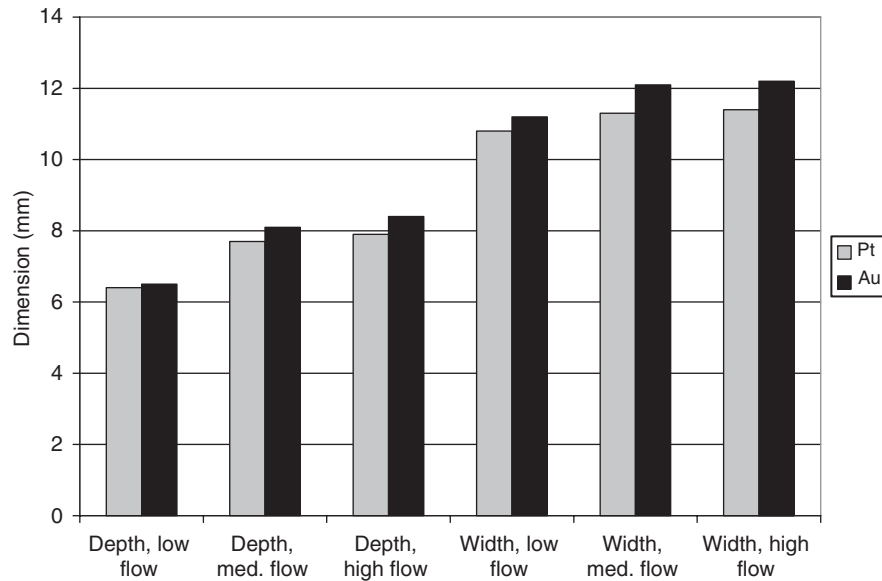


Figure 6. Comparison of lesion dimensions for the 8Fr catheter with 2.5 mm insertion depth.

Table V. Results from simulations with constant power algorithm. All values in the table are from simulations with the Pt electrode (results with Au and Cu electrode materials were similar).

Catheter size	Insertion depth	Flow type	Power (W)	Max tissue temp ($^{\circ}$ C)	Lesion width	Lesion depth
7Fr	0.75	low	3.24	68.4	8.1	4.1
7Fr	0.75	medium	6.14	83.8	8.2	5.3
7Fr	0.75	high	6.78	86.7	8.1	5.5
7Fr	1.25	low	2.47	63.3	7.6	4.1
7Fr	1.25	medium	4.93	77.3	8.1	5.4
7Fr	1.25	high	5.54	80.5	8.1	5.7
7Fr	2.5	low	1.51	58.1	6.9	4.5
7Fr	2.5	medium	3.18	67.6	7.9	5.8
7Fr	2.5	high	3.75	71.2	8.3	6.2
8Fr	0.75	low	10.03	79.6	11.0	5.5
8Fr	0.75	medium	15.35	92.5	10.2	6.5
8Fr	0.75	high	16.34	93.9	10.0	6.6
8Fr	1.25	low	8.35	73.3	10.6	5.5
8Fr	1.25	medium	13.30	87.3	10.4	6.7
8Fr	1.25	high	14.17	89.5	10.2	6.8
8Fr	2.5	low	6.30	66.6	10.2	6.1
8Fr	2.5	medium	10.83	81.3	11.0	7.5
8Fr	2.5	high	11.66	83.9	11.0	7.7

Note: All distance measurements are in mm.

were lesion widths in the simulations with the 8Fr catheter and 0.75 and 1.25 mm insertion depth, likely because reduced insertion depth limited the effects of electrode cooling. In addition, while there was a minor increase in difference in lesion dimensions between electrode materials with increasing flow and increasing insertion depth, again this difference was not significant.

As expected from prior studies [22–24], we also found that the lesion dimensions with the 8Fr catheter were larger than those with the 7Fr catheter (Tables III and IV), due to the longer electrode

length (10 vs. 4 mm, respectively) that facilitates greater convective cooling of the electrode–tissue interface allowing increased power application, as well as due to the larger electrode diameter which causes deeper penetration of RF current.

The Au electrode created only marginally larger thermal lesions than the Pt-Ir electrode for all combinations of flow, insertion depth, and catheter size, while there was no significant difference between lesion dimensions between the Au and Cu electrode simulations. This is likely because the difference in thermal conductivity between Au and

Cu ($\sim 1.3x$) is significantly smaller than the difference between Au and Pt-Ir ($\sim 4.5x$) (Table I).

There are two prior published ex vivo studies that compared Au- and Pt- electrodes. Both observed increases in lesion depth when using Au- electrodes, even though the differences were considerably larger than in our computer simulations. In one study by Lewalter et al., the lesion depth with Au electrodes was ~ 2 mm larger than platinum (4.9 ± 1.0 vs. 3.0 ± 0.8 mm), and in the other study by Simmons et al., lesion depth was 1.4 mm larger (5.8 ± 0.7 vs. 7.2 ± 1.4 mm). While the dimensions resulting from our models were in similar range, the greatest difference between lesion depth with a similar electrode as used in those ex vivo studies (7 Fr, 4 mm length) was 0.3 mm. There are many potential reasons for this discrepancy, among them incorrect material properties, geometry of the myocardial surface, and differences in power application algorithm. However, the small increase in lesion dimensions we found in the simulations could explain the lack of significant difference in efficacy found in clinical trials that have compared the two electrode materials [9, 10]. Therefore, while differences in electrode material properties may provide advantages in particular clinical situations, our modeling results suggest only potentially minor benefits.

Conclusions

Our computer modeling results show only minor increases in thermal lesion dimensions with electrode materials of higher thermal conductivity. These observed differences likely do not provide a significant advantage during clinical procedures.

References

1. Anfinsen OG, Aass H, Kongsgaard E, Foerster A, Scott H, Amlie JP. Temperature-controlled radiofrequency catheter ablation with a 10-mm tip electrode creates larger lesions without charring in the porcine heart. *J Interv Card Electrophysiol* 1999;3(4):343–351.
2. Demazumder D, Mirotnik MS, Schwartzman D. Comparison of irrigated electrode designs for radiofrequency ablation of myocardium. *J Interv Card Electrophysiol* 2001;5(4):391–400.
3. Petersen HH, Chen X, Pietersen A, Svendsen JH, Haunso S. Tissue temperatures and lesion size during irrigated tip catheter radiofrequency ablation: An in vitro comparison of temperature-controlled irrigated tip ablation, power-controlled irrigated tip ablation, and standard temperature-controlled ablation. *Pacing Clin Electrophysiol* 2000;23(1):8–17.
4. Pilcher TA, Sanford AL, Saul JP, Haemmerich D. Convective cooling effect on cooled-tip catheter compared to large-tip catheter radiofrequency ablation. *Pacing Clin Electrophysiol* 2006;29(12):1368–1374.
5. Ruffey R, Imran MA, Santel DJ, Wharton JM. Radiofrequency delivery through a cooled catheter tip allows the creation of larger endomyocardial lesions in the ovine heart. *J Cardiovasc Electrophysiol* 1995;6(12):1089–1096.
6. Yokoyama K, Nakagawa H, Wittkampf FH, Pitha JV, Lazzara R, Jackman WM. Comparison of electrode cooling between internal and open irrigation in radiofrequency ablation lesion depth and incidence of thrombus and steam pop. *Circulation* 2006;113(1):11–19.
7. Lewalter T, Bitzen A, Wurtz S, Blum R, Schlodder K, Yang A, Lickfett L, Schwab JO, Schrickel JW, Tiemann K, et al. Gold-tip electrodes - a new 'deep lesion' technology for catheter ablation? In vitro comparison of a gold alloy v.s. platinum-iridium tip electrode ablation catheter. *J Cardiovasc Electrophysiol* 2005;16(7):770–772.
8. Simmons WN, Mackey S, He DS, Marcus FI. Comparison of gold versus platinum electrodes on myocardial lesion size using radiofrequency energy. *Pacing Clin Electrophysiol* 1996;19(4):398–402.
9. Sacher F, O'Neill MD, Jais P, Huffer LL, Laborderie J, Derval N, Deplagne A, Takahashi Y, Jonnson A, Hocini M, et al. Prospective randomized comparison of 8-mm gold-tip, externally irrigated-tip and 8-mm platinum-iridium tip catheters for cavotricuspid isthmus ablation. *J Cardiovasc Electrophysiol* 2007;18(7):709–713.
10. Stuhlinger M, Steinwender C, Schnoll F, Winter S, Freihoff F, Wurtz S, et al. GOLDART - Gold Alloy Versus Platinum-Iridium Electrode for Ablation of AVNRT. *J Cardiovasc Electrophysiol* 2008;19(3):242–246.
11. Berjano EJ, Navarro E, Ribera V, Gorris J, Alio JL. Radiofrequency heating of the cornea: An engineering review of electrodes and applicators. *The Open Biomedical Engineering Journal* 2007;1:71–76.
12. Tungjitkusolmun S, Woo EJ, Cao H, Tsai JZ, Vorperian VR, Webster JG. Thermal-electrical finite element modelling for radio frequency cardiac ablation: Effects of changes in myocardial properties. *Med Biol Eng Comput* 2000;38(5):562–568.
13. Duck FA. Physical properties of tissue: A comprehensive reference book. London and San Diego: Academic Press, 1990.
14. Kreith F. The CRC handbook of thermal engineering. Vol. 4. Boca Raton, FL: CRC Press, 2000, pp 122–125.
15. Lide DR. CRC Handbook of chemistry and physics, 87th ed. Boca Raton, FL: Taylor and Francis, 2006.
16. Panescu D, Wayne JG, Fleischman SD, Mirotnik MS, Swanson DK, Webster JG. Three-dimensional finite element analysis of current density and temperature distributions during radio-frequency ablation. *IEEE Trans Biomed Eng* 1995;42(9):879–890.
17. Tsai JZ, Will JA, Hubbard-Van Stelle S, Cao H, Tungjitkusolmun S, Choy YB, Haemmerich D, Vorperian VR, Webster JG. In-vivo measurement of swine myocardial resistivity. *IEEE Trans Biomed Eng* 2002;49(5):472–483.
18. Tungjitkusolmun S, Vorperian VR, Bhavaraju N, Cao H, Tsai JZ, Webster JG. Guidelines for predicting lesion size at common endocardial locations during radio-frequency ablation. *IEEE Trans Biomed Eng* 2001;48(2):194–201.
19. Haemmerich D, Webster JG. Automatic control of finite element models for temperature-controlled radiofrequency ablation. *Biomed Eng Online* 2005;4(1):42.
20. Nath S, Lynch 3rd C, Wayne JG, Haines DE. Cellular electrophysiological effects of hyperthermia on isolated guinea pig papillary muscle. Implications for catheter ablation. *Circulation* 1993;88(4):1826–1831.
21. Haines DE. Biophysics of radiofrequency lesion formation. In: Huang SK and Wood MA, editors. Catheter ablation of

- cardiac arrhythmias. Philadelphia: Saunders/Elsevier, 2006, pp 3–20.
22. Blafox AD, Numan MT, Laohakunakorn P, Knick B, Paul T, Saul JP. Catheter tip cooling during radiofrequency ablation of intra-atrial reentry: Effects on power, temperature, and impedance. *J Cardiovasc Electrophysiol* 2002;13(8):783–787.
 23. Feld G, Wharton M, Plumb V, Daoud E, Friehling T, Epstein L. Radiofrequency catheter ablation of type 1 atrial flutter using large-tip 8- or 10-mm electrode catheters and a high-output radiofrequency energy generator: Results of a multicenter safety and efficacy study. *J Am Coll Cardiol* 2004;43(8):1466–1472.
 24. Otomo K, Yamanashi WS, Tondo C, Antz M, Bussey J, Pitha JV, Arruda M, Nakagawa H, Wittkampf FH, Lazzara R, et al. Why a large tip electrode makes a deeper radiofrequency lesion: Effects of increase in electrode cooling and electrode-tissue interface area. *J Cardiovasc Electrophysiol* 1998; 9(1):47–54.